Hybrid Simulation of the Seismic Response of Squat Reinforced Concrete Shear Walls

C.A. Whyte
University of California, Berkeley

B. Stojadinovic
Swiss Federal Institute of Technology, Zurich

SUMMARY:
Most industrial and nuclear energy facilities rely on squat reinforced concrete structural walls as their primary seismic lateral-force-resisting components. The walls commonly have an aspect ratio smaller than 0.5 and are designed to be thick for radiation shielding and blast and fire protection, resulting in a very high wall stiffness and strength. However, there is significant uncertainty associated with the behavior of these walls under earthquake loading, their failure modes, and their expected strengths and deformation capacities. Hybrid simulation is an effective experimental method to examine these issues: it enables simulation of the seismic response of squat and thick shear walls without the need to recreate the, often very large, mass associated with the rest of the prototype structure. A new method for hybrid simulation of the earthquake response of stiff specimens was developed and verified. Physical hybrid tests were performed on two large-scale squat reinforced concrete walls.

Keywords: hybrid simulation, reinforced concrete, squat wall, shear strength

1. INTRODUCTION

Most industrial and nuclear energy facilities are low-rise reinforced concrete buildings with a large footprint. Generally, their structural walls are used as the primary seismic lateral-force-resisting components. In nuclear structures, the walls are designed to have as few openings as possible to prevent radiation leaks. This design is also typical in industrial structures to simplify construction; few access points and windows are required. Thus, the resulting structural systems are comprised of long walls with a relatively short height. Nuclear facility walls are designed to be thick for radiation shielding as well as blast and fire protection. Similar thick walls are also found in industrial structures. The combination of a squat and thick wall geometry results in a high initial wall stiffness, leading to structures that are very stiff, i.e. have a very short fundamental mode vibration period. Consequently, the seismic shear demands on such structures can be very high. Most design codes define squat walls to have aspect ratio ≤ 2.0. In nuclear structures, this aspect ratio is commonly ≤ 0.5. The squat geometry of these walls causes them to fail in shear or sliding shear. These failure modes are not preferred since they can occur suddenly and after very little elastic deformation.

Shear walls in nuclear structures are designed to attain an "essentially elastic" limit state in a Design Basis Earthquake (DBE, 10% in 50 probability of exceedance). This means the walls are designed such that they will only experience a slight amount of yielding in a DBE event. However, this approach is potentially problematic for a very stiff structural element. The displacement ductility demand for a very stiff structure may be very large even if the structure yields only slightly (Chopra, 2007). Therefore, it is important to investigate behavior of the stiff shear walls in the case that the structure experiences an earthquake ground motion that introduces much larger seismic shear demands than those considered in design. To further complicate matters, current building code equations have been shown to generally overpredict the peak shear strength of squat reinforced concrete shear walls, and do so significantly in some cases. Gulec (2005) created a database from the results of tests from

352 squat shear walls (aspect ratio ≤ 2.0). The large scatter in the ratio of predicted strength to measured strength for the 150 rectangular-section shear walls in his database is shown below in Fig. 1. The authors reviewed design equations from ACI 318-05 Chapter 21, ACI 318-05 Chapter 11, Barda et al. (1977), ASCE/SEI 43-05, and Wood (1990). In the worst cases, the design code equations overpredict the peak shear strength of squat walls by a factor as large as 3.

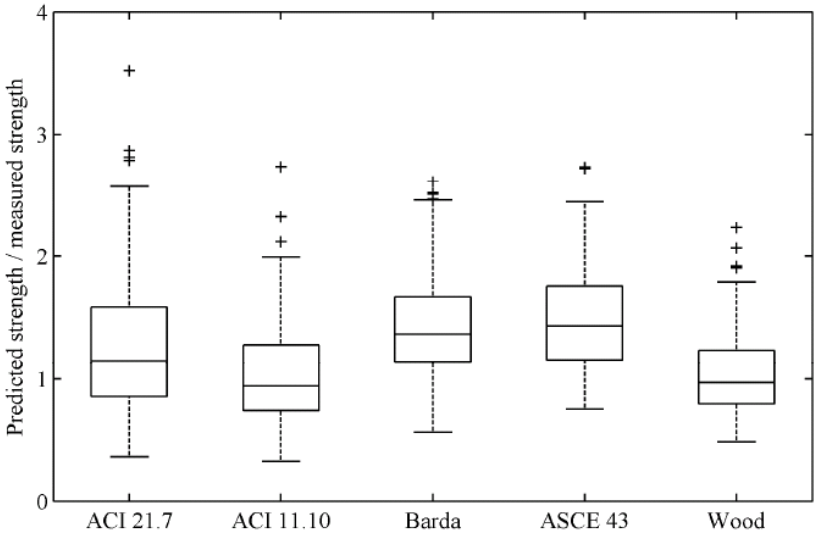

Figure 1. Ratio of Predicted to Measured Squat Wall Strength (Gulec 2009)

This scatter in the shear wall capacity data, the difficulty of predicting the seismic shear demand for such stiff structural elements, and the potentially very serious consequences of sudden failure motivate this study to better understand the behavior of squat reinforced concrete shear walls. The NEES-R project team assembled to tackle this task comprises member from the University at Buffalo, University of Washington and University of California, Berkeley. Since the data obtained by Gulec came from many experimental sources with a variety of testing parameters, the University at Buffalo team is investigating the behavior of squat walls with varying aspect ratios and reinforcement ratios using standard quasi-static loading and a consistent test setup for all cases. The University of Washington team is focusing on finite element modeling. The University of California Berkeley team conducted two hybrid simulations of earthquake response to compare to the quasi-static test results and validate the finite element models. The hybrid simulations are described in this paper.

2. ENCODER CONTROL FOR HYBRID SIMULATION OF A STIFF SPECIMEN

A hybrid model consists of a physical portion and a numerical portion. The structural components whose behavior is well-understood are typically modeled numerically and the components that are not well-understood or expect significant nonlinear behavior are modeled physically. A displacement control strategy is most commonly implemented, as summarized in Fig. 2.

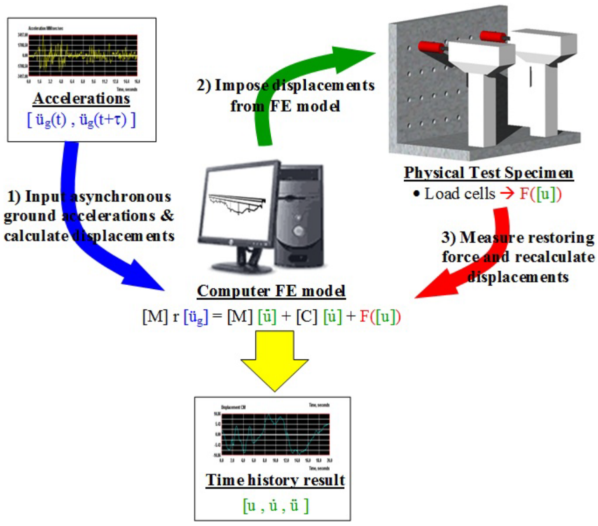

Figure 2. Hybrid Simulation in Displacement Control

The equation of motion for the hybrid model is discretized in time and given as Eqn. 1 below:

$$M\ddot{u}_{i+1} + C\dot{u}_{i+1} + R(u_{i+1}) = -MB\ddot{u}_{g,i+1} \tag{1}$$

where M is the mass hybrid model matrix, C is the viscous damping hybrid model matrix, and R is the nodal restoring forces vector, assembled from the restoring forces from the physical and the computer portions of the hybrid model. u is a vector of displacements at each degree of freedom, $\dot{u}$ is a vector of the velocities at each degree of freedom, and $\ddot{u}$ is a vector of the accelerations at each degree of freedom. Matrix B is the ground acceleration transformation matrix and $\ddot{u}_g$ is the vector of recorded ground accelerations.

The earthquake acceleration record is provided to the computer finite element model at discrete time steps. At each step, the acceleration is entered into the equation of motion, which represents the structural behavior. A numerical integration technique is employed to solve the equation of motion for a target displacement that the physical test specimen must move to. The actuator in the laboratory applies this target displacement to the physical specimen and the load cell records the restoring force. This restoring force is entered into the governing equation of motion for the structure, and then the equation is re-solved at the next time step. This process repeats throughout the duration of the ground motion as the response of the structure is recorded.

The high stiffness of the squat shear walls poses a challenge to this conventional hybrid simulation displacement control approach. For a stiff specimen, a small increment in displacement corresponds to a large increment in force. Large-scale models of squat walls are stiff and strong: testing to failure often requires forces in excess of 2,224 kN (500 kips), which in turn requires use of one very large actuator or a system of two or more conventional 979 kN (220 kips) actuators. In order to move the specimen smoothly from step to step, large force increments must be avoided. A large force increment could cause the specimen to suddenly change its failure mode or fail completely. This could produce misleading results since the change in specimen behavior would be a result of a poorly-controlled simulation instead of a realistic behavior. Another possible problem with a stiff specimen is that small displacement errors will lead to significant force errors in the simulation, and possibly to instability of the simulation setup. If the specimen is extremely stiff, the required displacement increment to achieve a reasonable-size force increment may become so small that it is on the order of the tolerance that the laboratory system can control.

This problem can be overcome by using a very high precision displacement encoder to feedback displacements in the PID loop. The *nees@berkeley* Equipment Site acquired a displacement encoder with a step resolution of 10 microns (0.0004 in). It was successfully included in the actuator control loop to feedback small enough displacement increments to create smooth loading of the squat shear wall specimen. The software used for the hybrid simulations included finite element software, Open System for Earthquake Engineering Simulation (OpenSees, 2012), and hybrid simulation framework, Open-source Framework for Experimental Setup and Control (OpenFresco, 2012), both developed at Berkeley.

3. HYBRID MODEL AND PHYSICAL SPECIMENS

The hybrid simulation tests involved applying varying levels of a ground motion excitation to a simplified hybrid model of a typical nuclear power plant structure. This hybrid model was a combination of a physical squat shear wall specimen with a computer model to represent the mass of a typical nuclear structure, tributary to this wall. The mass was adjusted to match a 0.14 second fundamental mode vibration period, selected based on a Candu Reactor prototype (Huang and Whittaker, 2008; Huang et al, 2009). Implementing the mass in the numerical model allowed for the seismic response of the hybrid model to match that of the entire structure without having to physically add mass to the shear wall specimen. The authors considered numerically modeling the remaining lateral force resisting system of the building (the other shear walls). This approach was not pursued because the outcome of the simulation would depend on an accurate estimate of the stiffness of the numerically modeled walls. If the walls that were analytically modeled were stiffer than the physical specimen, they would not fail and would take all the force when the specimen began to soften. Alternatively, if the analytical walls were softer than the physical specimen, they would fail too early and overload the physical specimen.

Two nominally identical squat reinforced concrete shear walls, referred to as Wall 1 and Wall 2, were tested at the *nees@Berkeley* laboratory. The shear wall specimens were 20 cm (8 in) thick models of a prototype 1 m (36 in) thick structural wall typically found in nuclear power plant structures. The walls were 3 m (10 ft) long and 1.65 m (5 ft, 5 in) tall to the height of the actuator axis (aspect ratio 0.54). They had a 0.67% horizontal and vertical wall reinforcement ratios with bars placed in two curtains. The concrete mix design had a target compressive strength of 34.5 MPa (5000 psi). Photographs of the walls are shown in Figure 3. The blue steel plate is used to distribute the load from the actuator (located on the right side of the wall) across the top of the wall. The high precision displacement encoder measures the displacements of the wall at the top center of the specimen with reference to a frame on the back side of the wall. This relatively stiff frame is embedded in the foundation of the specimen to eliminate the effect of any deformations at the interface between the specimen and the laboratory test floor. In addition to traditional instrumentation including strain gages and Novotechnic potentiometers, Krypton system targets were used on a portion of the front side of the wall to monitor displacements in the surface plane, shown in Fig. 3. Additionally, for the Wall 2 test, an image correlation software, VIC-2D 2009, was used to map strains (Correlated Solutions, 2009). A random pattern of dots was drawn on the wall, and high resolution cameras were used to photograph the pattern throughout the test. The VIC-2D software determined strains by tracking the motion of the pattern of dots in a sequence of images.

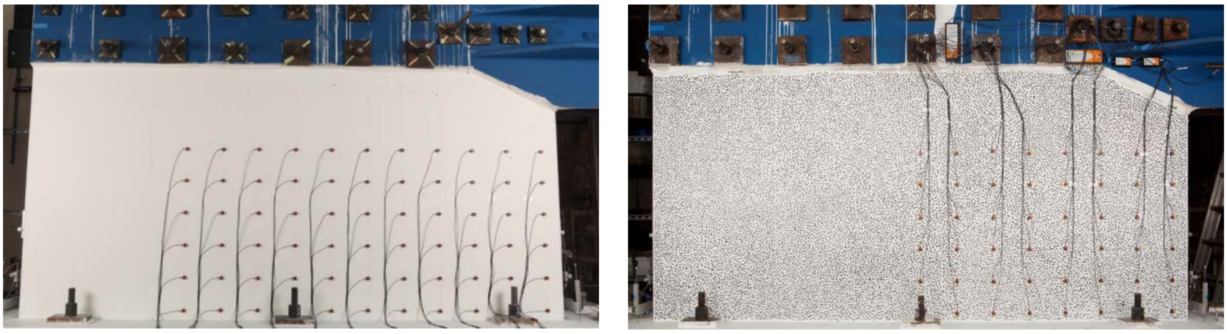

Figure 3. Wall 1 and Wall 2 Specimens

The site for the nuclear structure considered for the hybrid simulation tests was a Western US rock site at Diablo Canyon Nuclear Power Plant in San Luis Obispo County, CA, USA. Huang and Whittaker (Huang and Whittaker, 2008; Huang et al, 2009) obtained the DBE spectrum for this site from the Nuclear Regulatory Commission (NRC). They matched 30 ground motions to the DBE spectrum over a wide range of periods using seed motions from the PEER NGA Database (PEER, 2012). Since the fundamental period of the hybrid model is expected to elongate as the shear wall specimen is damaged during the simulation, the ground motion that best matched the DBE spectrum in the 0.14 s to 0.3 s range of periods was selected for the hybrid simulation. This motion was the 1999 Kocaeli, Turkey earthquake.

4. TEST PROCEDURE

A stiffness pre-test was performed on each wall specimen before the start of hybrid simulations. A very small saw-tooth displacement-controlled motion was imposed, with forces limited to +/-444.8 kN (+/-100 kips). Because of the high stiffnesses of the walls, the forces were initially very difficult to control and fluctuated within +/-444.8 kN (+/-100 kips). The stiffness of Wall 1 was found to be about 840.6 kN/mm (4800 kips/in). This value was used to determine the mass in the numerical model to achieve the fundamental vibration period of 0.14 s for the hybrid model. Inspection of the specimen after this pre-test revealed several hair-line diagonal cracks. The pre-test for the Wall 2 specimen resulted in a similar stiffness and crack pattern.

Next, a free vibration pre-test was performed to assess the damping in the system due to errors in the control loop and to determine the appropriate velocity for the simulation. The forces were also kept below +/-444.8 kN (+/-100 kips) for this test. Since the clevises of the actuator slip slightly on load direction reversal, the simulation was conducted using a constant actuator velocity model in order to limit control errors. A velocity of 0.254 mm/s (0.01 in/s) was selected. With this velocity, the free vibration exhibited just about 0 damping. Thus, the desired 2% damping was implemented directly in the numerical model.

The Wall 1 hybrid model was tested using increasing levels of the ground motion as follows: an operational basis earthquake (OBE), a DBE, and a beyond design basis earthquake (BDBE), followed by a DBE aftershock. The Wall 2 hybrid model was tested starting with an OBE, followed by a BDBE, followed by two DBE aftershocks. At the end of both simulations, the walls had lost most of their strength. The authors decided that it would not be safe to perform further ground motion simulations. Instead, the walls were broken using quasi-static single-cyclic saw-tooth motions to +/-2.54 cm (+/-1 in) and then +/-3.81 cm (+/-1.5 in) peak displacements.

The OBE, DBE, and BDBE ground motion levels were chosen based on the expected behavior of a nuclear structure in these events. The OBE motion targeted about 1/3 of the yield force, the DBE motion targeted about 2/3 of the yield force, and the BDBE motion targeted pushing the wall beyond peak strength. The results of a cyclic test of a nominally identical squat wall specimen at University at Buffalo were used to determine the target force levels for the ground motions (Rocks et al, 2011). A single-degree-of-freedom oscillator non-linear model was developed in OpenSees to help predict the wall behavior for different earthquake scaling values. This model worked well in the essentially elastic response range, but proved unreliable after the wall began to accumulate damage. In the Wall 1 hybrid simulation, the DBE motion applied after the OBE motion was smaller than desired (scaling factor 0.1052). The scaling factor was increased to 0.1407 and the test was repeated to achieve the desired response. Then the BDBE motion was chosen as three times DBE. The same scaling values were used for the Wall 2 hybrid simulation and produced the expected response levels. Scaling factors for the 1999 Kocaeli, Turkey earthquake record are summarized in Table 1.

Table 1. Ground Motion Scaling Factors

GM Level	Scaling Factor
OBE	0.05263
DBE	0.1407
BDBE	0.4221

5. RESULTS

During the OBE simulations, both shear wall specimens developed minor diagonal shear-induced cracking at about 45 degrees, distributed throughout the wall web. This indicated that the loading plate distributed the forces well along the length of the wall. The shear cracks grew during the Wall 1 DBE 1 simulation and during the beginning of the Wall 2 BDBE simulation. Figs. 4 through 6 show ε_{yy} strains measured on the surface of the Wall 2 specimen during the BDBE simulation using high-resolution still image correlation. Fig. 4 was recorded at the beginning of the BDBE simulation. Light shear cracking is evident throughout the wall web along with some flexural cracks near the lower corners of the wall. As the BDBE motion progressed, the flexural behavior mode became more dominant, as shown in Fig. 5. Finally, the cracks in the lower left and right corners of the wall propagated along the entire base of the wall and the wall began to slide along a narrow sliding zone. This is shown in Fig. 6. After the wall has slid to the point when the vertical reinforcement picked up some force in dowel action, the flexural cracks continued to develop. This is apparent in Fig. 6 as well. Not visible in this figure, but shown in Fig. 7, is local buckling of the vertical wall reinforcement and opening of the hooks of the horizontal wall reinforcement induced by a combination of sliding and flexure. This picture was taken at the end of the test when the broken concrete pieces had been removed.

For the purpose of wall displacement analysis, the sliding zone is defined as the 7.62 mm (3 in) narrow zone at the interface between the wall and its foundation. This zone includes the primary flexural crack along which sliding occurred, the first horizontal reinforcing bar, and a portion of the length where the vertical reinforcing bars acted as dowels on the sliding surface. The height of the sliding zone matches the attachment location of the first level of vertical and horizontal displacement measurement instruments. Pairs of vertical and horizontal displacement potentiometers were installed at the left and the right edges of the wall at 7.62 cm (3 in), 22.86 cm (9 in), and 48.26 cm (19 in) above the foundation. A separate system of displacement potentiometers, arranged in a square pattern along the back of the wall, was used to measure shear deformations.

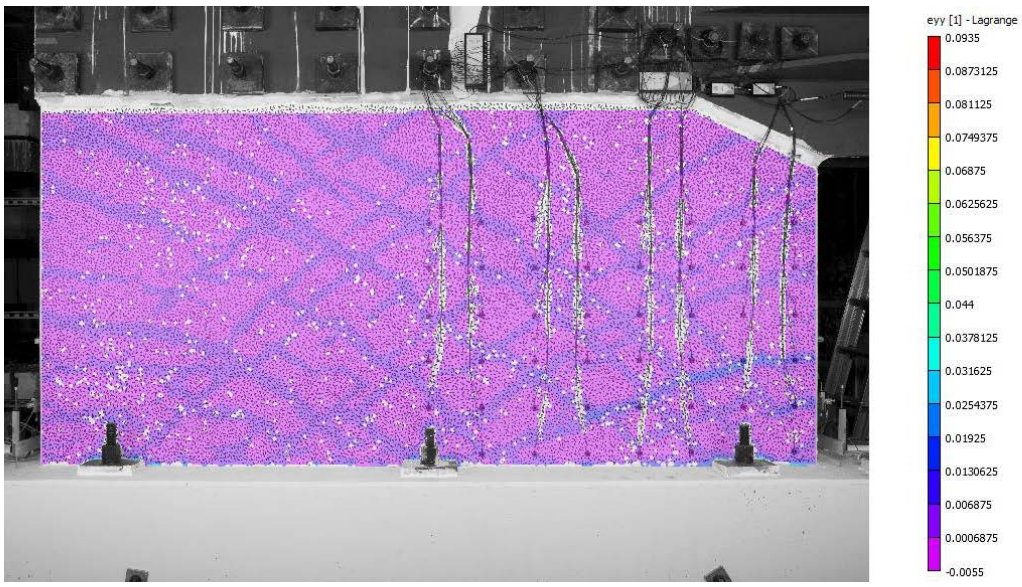

Figure 4. Wall 2 Shear and Flexural Cracking at Start of BDBE Motion

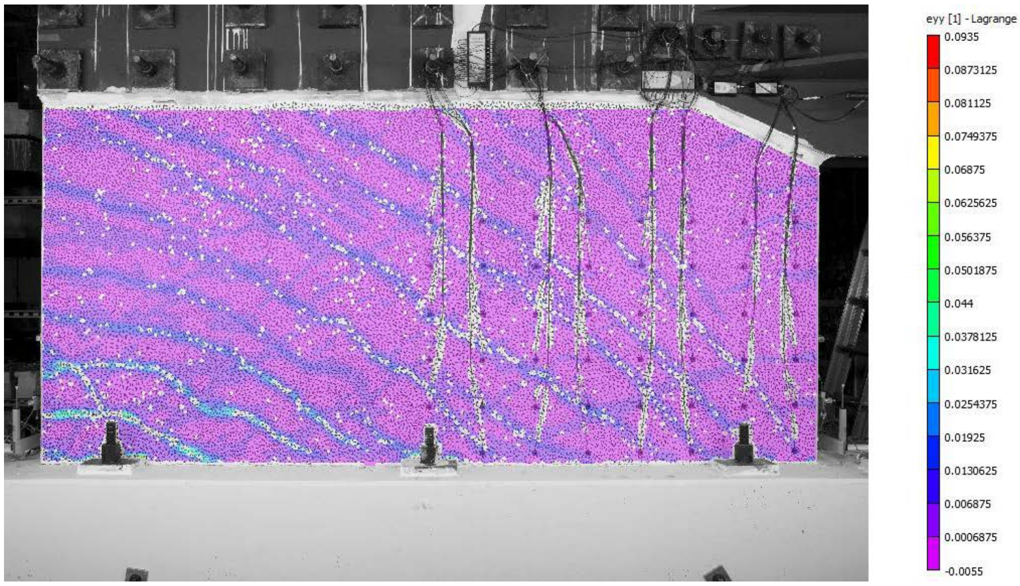

Figure 5. Wall 2 Development of Flexural Cracks during BDBE Motion

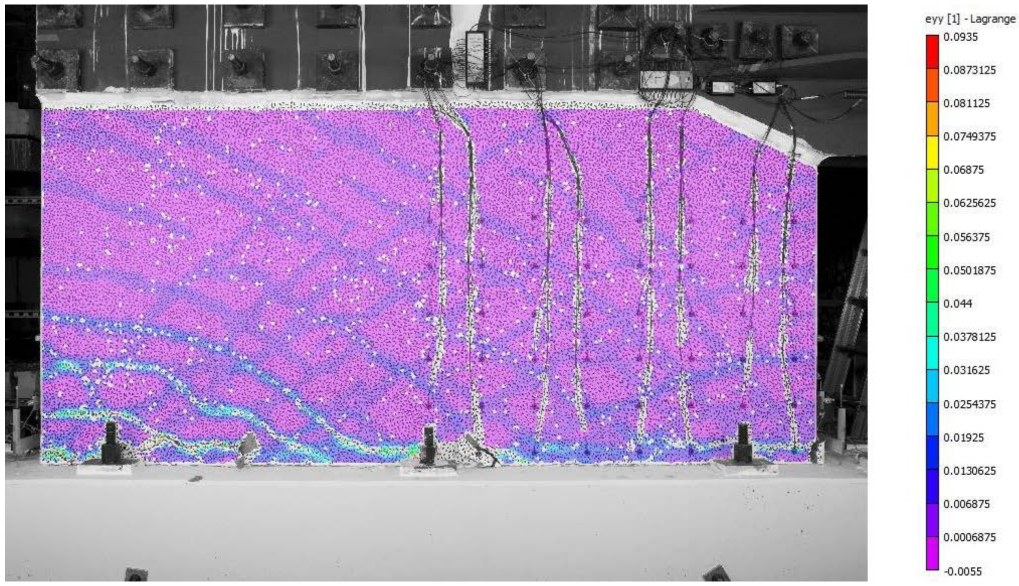

Figure 6. Wall 2 Continued Development of Flexural Cracking and Sliding during BDBE Motion

Figure 7. Local Buckling of Vertical Bars and Opening of Hooks

The contributions to the total displacement of the shear wall specimens were divided into the following four portions: displacements 1) due to flexural rotation of the sliding zone; 2) due to sliding in the sliding zone; 3) due to flexure of the rest of the wall; and 4) due to shear deformation of the rest of the wall. These displacement contributions to the total displacement during the Wall 2 BDBE motion simulation are shown in Fig. 8. All displacement measurements were recorded relative to the foundation, so only the motion due to wall deformation is captured.

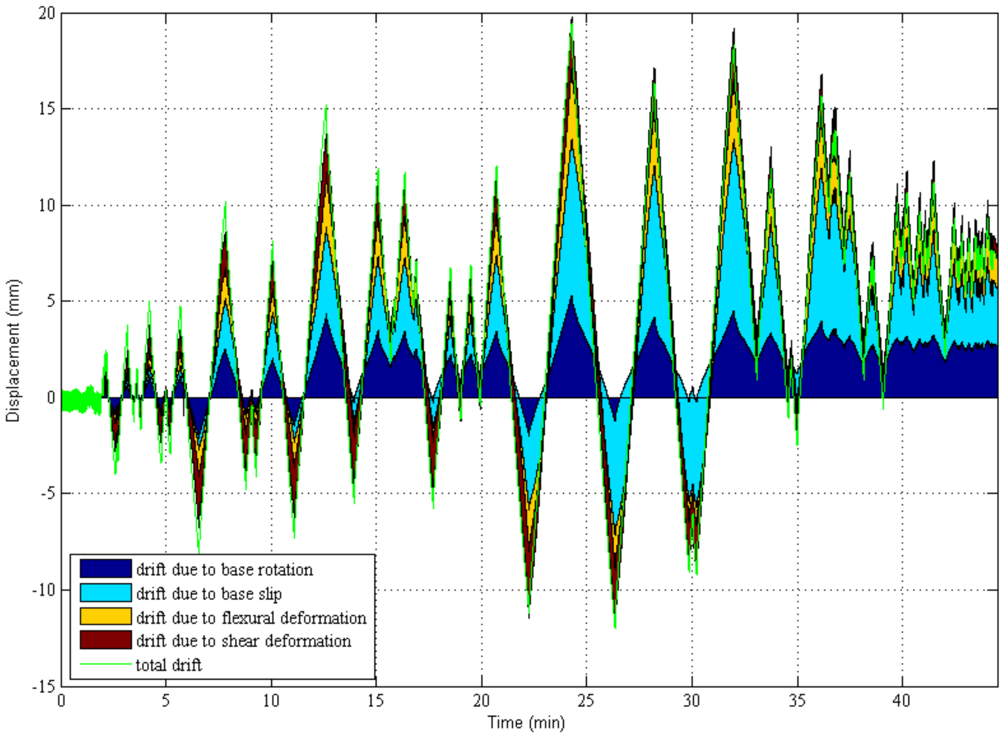

Figure 8. Wall 2 BDBE Displacement Contributions

During the Wall 2 BDBE motion, the contribution of wall shear deformation to the total deformation is larger at the beginning of the motion and diminishes after the wall attains its peak strength. The contribution of wall flexural deformation above the sliding zone is fairly constant. Most of the wall flexural motion comes from the base rotation in the bottom 7.62 cm (3 in) region of the wall. Contributions occurring in this sliding zone begin to dominate the deformation of the wall as soon as the intense cycles of the ground motion start. The portion due to flexure in the sliding zone remains fairly constant, while the portion due to base slip grows. The sum of the displacement contributions from these four sources is slightly less than the total displacement at the beginning of the BDBE motion. This is due to the slip in the actuator clevises, which comprises a larger percentage of the total displacement at very small displacement levels than it does later in the test.

The force-drift ratio plots for corresponding ground motions in the Wall 1 and Wall 2 tests are shown in Fig. 9. The response of both shear wall specimens to the selected ground motions was asymmetric. The authors suspected this was the result of the nature of the ground motion and not an asymmetry in the test setup. In order to confirm this, the ground motion direction was reversed for the second hybrid simulation by changing the algebraic sign of the acceleration array. The signs of the force and drift ratio data for Wall 2 were negated to facilitate comparison between the two specimens in Fig. 9. The plots are shown in the order that the hybrid tests were performed: first the OBE motions are compared, then the BDBE motions, then a DBE aftershock, and finally the displacement cycles. The nominal shear strength of the wall according to ACI 318 Chapter 21.7 is 2965 kN (666.6 kips). This is included as a black line in the BDBE plot. The peak force for Wall 1 was 1633.1 kN (367.1 kips) and the peak force for Wall 2 was 1709.9 kN (384.4 kips).

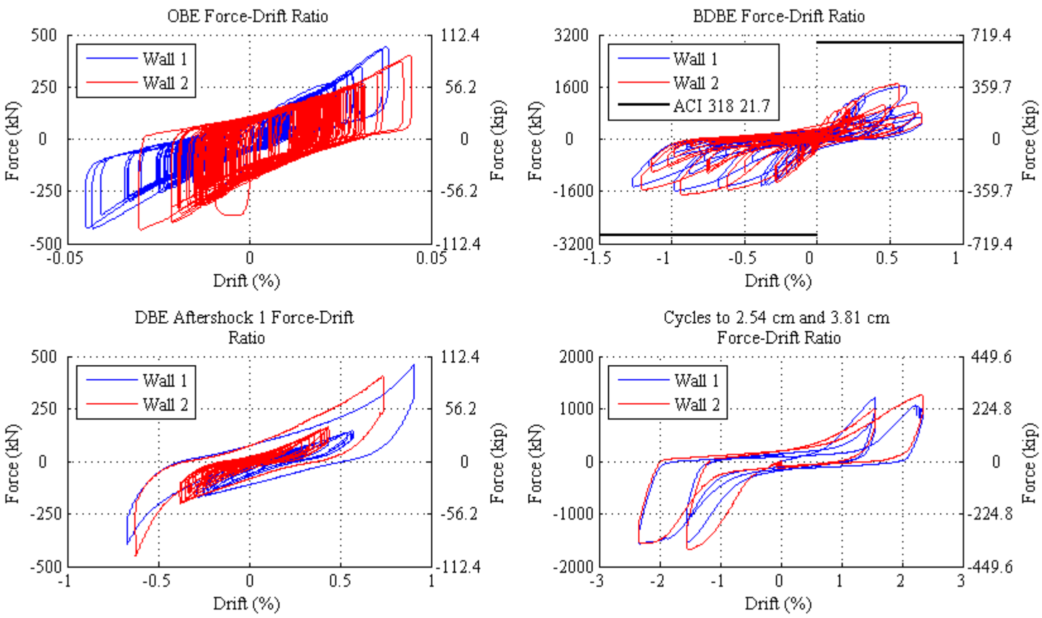

Figure 9. Wall 1 and Wall 2 Force-Drift Ratio Comparison for Ground Motion Test Sequence

The force-deformation responses of Wall 1 and Wall 2 specimens during the BDBE hybrid simulations are very similar. In Wall 2, the BDBE motion was applied directly following the OBE, whereas in Wall 1, the sequence was OBE, then DBE, and then BDBE. Wall 2 developed a slightly higher resistance at a slightly smaller drift ratio since it was stiffer than Wall 1 at the time the BDBE motion was applied. Shown in Fig. 9 (most evident in the BDBE motion) is a sudden drop in specimen resistance when the direction of the actuator motion changes. This is due to the slip in the actuator's clevises. When the actuator is pushing the specimen, the clevis gaps are closed. When the direction of motion changes, first the clevis gaps must open and then the specimen begins to move. As the clevis gaps are opening, the force on the wall is decreasing but the wall itself is not yet moving.

6. CONCLUSIONS AND FUTURE WORK

Displacement control hybrid simulation using a high precision encoder for displacement feedback is an effective way to perform large-scale hybrid testing of stiff specimens. This new method is useful to address the shortcomings in understanding the dynamic behavior of these types of specimens.

Two squat reinforced concrete shear wall specimens were tested at UC Berkeley. The goal of these tests was to obtain the seismic response of these walls to ground motion excitation. The tests were conducted using the hybrid simulation method. The difference between the tests was the sequence of the applied ground motion intensity. Both tested walls initially experienced shear and flexural deformations. However, as the displacement demands grew, the flexural cracks from each end of the wall joined to form a continuous crack along the interface between the wall and its foundation. Sliding in the narrow zone surrounding this crack initiated immediately and grew to dominate the response of the seismic walls. The eventual failure mode of both tests specimens was sliding shear failure.

The behavior of the squat walls obtained by hybrid simulations presented in this study will be compared to quasi-static cyclic test data for squat wall specimens with the same design parameters tested at University at Buffalo to determine whether quasi-static cyclic testing effectively captures the dynamic behavior of stiff squat walls. This data will also serve to calibrate both the finite element and design models for squat reinforced concrete walls.

AKCNOWLEDGEMENT

Support for this project was provided by NSF NEES-R grant CMMI-0829978. Any opinions, findings, and conclusions expressed herein are those of the author(s) and do not necessarily reflect the view of the National Science Foundation.

REFERENCES

American Concrete Institute (ACI) Committee 318-08. (2008). Building Code Requirements for Structural Concrete and Commentary (ACI 318-08). Farmington Hills, MI.

American Society of Civil Engineers (ASCE). (2007). Seismic Design Criteria for Structures, Systems, and Components in Nuclear Facilities (ASCE/SEI 43-05). ASCE, Reston, VA.

Barda, F., Hanson, J. M. and Corley, W. G. (1977). Shear strength of low-rise walls with boundary elements. *Reinforced Concrete Structures in Seismic Zones*. SP-53, American Concrete Institute, Farmington Hills, MI, pp. 149-202.

Chopra, A. (2007). Dynamics of Structures: Theory and Applications to Earthquake Engineering. 3rd edition, Chapter 7, Pearson, Prentice Hall.

Correlated Solutions. (2009). VIC-2D. http://www.correlatedsolutions.com/index.php/products/vic-2d-2009.

Gulec, C. K. (2005). Ultimate Shear Strength of Squat Rectangular Reinforced Concrete Walls. MS Thesis, Department of Civil, Structural and Environmental Engineering, State University of New York at Buffalo, Buffalo, NY.

Huang, Y.N. and Whittaker, A. S. (2008). Performance Assessment of Conventional and Base-Isolated Nuclear Power Plants for Earthquake and Blast Loadings. *Technical Report MCEER-08-0019*. University at Buffalo, State University of New York.

Huang, Y. N. et al. (2009). Assessment of Base-Isolated Nuclear Structures for Design and Beyond-Design Basis Earthquake Shaking. *Technical Report MCEER-09-0008*. University at Buffalo, State University of New York.

OpenFresco. (2012). Open Framework for Experimental Setup and Control. http://openfresco.neesforge.nees.org.

OpenSees. (2012). Open System for Earthquake Engineering Simulation. http://opensees.berkeley.edu.

PEER NGA Database. (2012). http://peer.berkeley.edu/peer_ground_motion_database.

Rocks, J. F., Luna, B. N., and Whittaker, A. S. (2011). Seismic Response of Low Aspect Ratio Reinforced Concrete Shear Walls. *SMiRT 21*, November 6-11, 2011, New Delhi, India.

Wood, S. L. (1990). Shear Strength of Low-Rise Reinforced Concrete Walls. *ACI Structural Journal*. **Vol. 87:1**, 99-107.